16

Investigation of Super-Lift Multilevel Inverter Using Water Pump Irrigation System

Johny Renoald Albert[1], Premkumar K.[2], Vanchinathan K.[3], Nazar Ali A.[2]*, Sagayaraj R.[4] and Saravanan T.S.[2]

[1]Department of Electrical and Electronics Engineering, Vivekanandha College of Engineering for Women, Namakkal, Tamil Nadu, India
[2]Department of Electrical and Electronics Engineering, Rajalakshmi Engineering College, Chennai, Tamil Nadu, India
[3]Department of Electrical and Electronics Engineering, Velalar College of Engineering and Technology, Erode, Tamil Nadu, India
[4]Department of Electrical and Electronics Engineering, Muthayammal Engineering College, Tamil Nadu, India

Abstract

The most significant development in DC-to-DC power conversion systems is the positive output voltage-lift method. The topology exists in two sorts such as super-lift and double-lift technique. Double-lift converter functions successfully DC-to-DC converter. The developed approach employs the invention of a super-lift multilevel method, which may minimize the number of recurring components when compared to the traditional sort of weird inverter. In this point, a new approach of single-source super-lift multilevel inverter (SLMLI) is proposed with concentrator solar module, which can perform the necessary voltage conversion applied in water pump irrigation using agricultural field. Designing a new SLMLI applied with PSO algorithm is also capable of determining the desired value of harmonics value performed with necessary power conversion. Solar water pumping systems are integrated in motor load; it has series connected to generate the required system load voltage, which is supplied by the availability of solar irradiation. Results present modified SLMLI with submersible water pump that helps to save the fuel and electricity cost,

**Corresponding author*: nazarali.a@rajalakshmi.edu.in

A. Chitra, V. Indragandhi, and W. Razia Sultana (eds.) Smart Grids and Green Energy Systems, (247–262)
© 2023 Scrivener Publishing LLC

10.1002/9781119872061.ch16, Downloaded from https://onlinelibrary.wiley.com/doi/10.1002/9781119872061.ch16 by Tsinghua University Library, Wiley Online Library on [05/11/2022]. See the Terms and Conditions (https://onlinelibrary.wiley.com/terms-and-conditions) on Wiley Online Library for rules of use; OA articles are governed by the applicable Creative Commons License

when compared to equivalent use of a diesel-operated water pump. The performances at various operating conditions are analyzed using MATLAB/Simulink and hardware-based result.

***Keywords*:** PV (photovoltaic), PSO (particle swarm optimization), SLMLI (super-lift multilevel inverter), submersible water pump, THD (total harmonic distortion)

16.1 Introduction

The concentrator solar photovoltaic (SPV) energy is one of the best alternate remedies or solutions for the rapid reduction of nonrenewable resources. The SPV energy is free and enormous, highly beneficial, and economically viable to many industrial applications [1]. Nonrenewable resources such as coal, petroleum, and natural gas are the primary sources of energy, but they will be depleted in a few decades. It also leads to environmental problems such as CO_2 emissions and the environmental impact [2]. Nowadays, water pumping is drawing huge attention among all the applications of PV module. To enhance the efficiency of concentrator SPV system, it is operated based on standard test condition [3]. Direct current converters are used to convert one level to another DC required level. Double-lift converters are mainly focused to enhance the DC-to-DC output voltage [4]. The positive output voltage at any required level attainments depends upon positive input DC source voltage. Voltage-lift performance is a standard scheme that is widely applied in electronic circuit design [5]. The multilevel converter employs power semi-conversion devices from lower DC voltage sources to generate an almost sinusoidal waveform of the staircase [6]. The main objective of the proposed system is to reduce the complexity of the multilevel inverter with reduced switches and diode sizes called as super-lift Luo inverter [7]. Inversion technology operates on vital mostly used in residential, domestic, electrical vehicles, and renewable energy systems. The proposed super-lift converter is put forth for PV concentrator module to apply water pump irrigation system. PV concentrate water pump system can operate all kinds of electric water pumps with applications ranging from irrigation to residential requirements [8]. A stand-alone PV system is provided for water pumping irrigation technology that has been constantly developed since the early 1980s.

In India, there are three primary solar water pumping configurations. Brushless DC pump, DC positive displacement pump, and AC centrifugal pump are all examples of brushless DC pumps. Submersible irrigation

10.1002/9781119873761.ch16, Downloaded from https://onlinelibrary.wiley.com/doi/10.1002/9781119873761.ch16 by Tsinghua University Library, Wiley Online Library on [05/11/2022]. See the Terms and Conditions (https://onlinelibrary.wiley.com/terms-and-conditions) on Wiley Online Library for rules of use; OA articles are governed by the applicable Creative Commons License

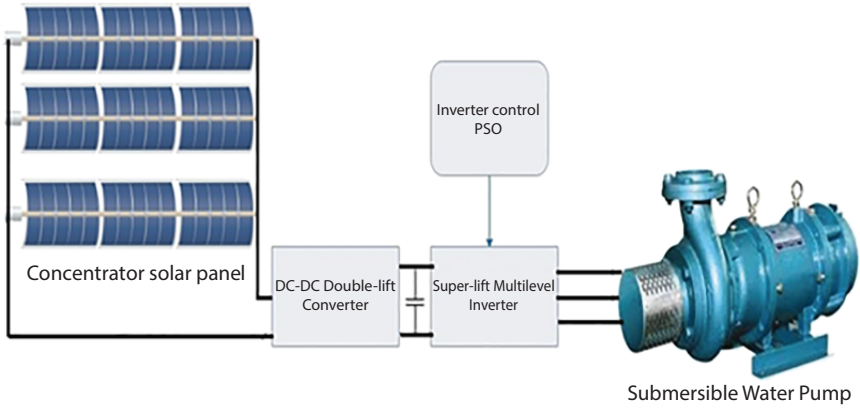


Figure 16.1 Block diagram for concentrator SPV super-lift Luo converter fed submersible motor drive.

water pumps can also be used in conjunction with drip irrigation systems to maximize the benefits of this setup [9]. Submersible pumps have the benefit of being totally submerged, including the engine. Water pumps are also more efficient since it is simply had to push water and do not have to suck it. The sum amount of solar array size necessary to operate the connected pump is known as a standard concentrator solar water pumping system. A number of solar modules are linked in series in each solar array. The integrated AC submersible pumps are connected to pull the water and feed it into delivery pipes, and the electrical energy from the complete array is controlled and directly adjusted by them [10]. These low-power submersible pumps make it possible to create a low-cost solar pumping system for a deep well. Figure 16.1 shows the suggested approach, which requires a 0.5-kWp solar water pump for the water pumping system. The unit is capable of extracting and pumping 20,000 to 25,000 liters of water per day from a source up to 3–5 meter deep. MATLAB/Simulink was used to assess the performance and measurement overall system output, and the prototype module for freestanding solar PV systems uses hardware-based results.

16.2 Proposed System Configuration

Small and marginal farmers are at danger economically due to a sparse electricity associated with the increased regularity of mountain rain and the prevalence of expensive diesel pumping. A complex mix of issues,

10.1002/9781119873266.ch16, Downloaded from https://onlinelibrary.wiley.com/doi/10.1002/9781119873266.ch16 by Tsinghua University Library, Wiley Online Library on [05/11/2022]. See the Terms and Conditions (https://onlinelibrary.wiley.com/terms-and-conditions) on Wiley Online Library for rules of use; OA articles are governed by the applicable Creative Commons License

such as global warming, competitive land usage, and a lack of basic infrastructure, is posing new difficulties to India's vast agricultural population. Then, there is power, which is especially difficult for farmers in rural locations. The configuration consists of PV module feeding the power to Luo converter, and super-lift inverter employed with submersible water pump work out with MATLAB/Simulink platform [11]. Submersible pumps are used to choose the outfall area and also connect the hose up to the pump. This prototype module control with PIC microcontroller chosen for its PWM control ability and hasty convergence [12]. This chapter generally focused on reducing the number of switches and DC sources used. We reduce the greater number of losses; voltage dropped across the switch. Design, control, and operation of each stage are elaborate individually as following section.

16.3 Design of Concentrator SPV Array

To determine the amount of water used, multiply the width of the yard by the length of the yard in feet to obtain the number of square feet. The water is driven by a 0.5-kW, 50-Hz submersible water pump that is powered by the SPV array. To compensate for motor and inverter losses, the SPV array rating is somewhat greater than the pump motor rating [13]. A SPV is created by linking 72 cell SPV modules in series with an open circuit voltage of 24 V and 72 cell SPV modules in sequence with a short circuit current of 1.5 A. As shown in Table 16.1, the voltage and current achieve their MPP at approximately 81% of open circuit voltage and 90% of ISC, correspondingly. There are various sub-series circuits in positive output super-lift converters [14, 15]. Stage by stage, the circuits' voltage gains grow in geometrical series. Figure 16.2 depicts a basic positive output double-lift or re-lift converter. When switch S is turned on, the comparable circuits are shown in Figure 16.2a, and when switch S is turned off, the corresponding circuits are shown in Figure 16.2b. When the primary switch S is switched off, the inductor L1 and capacitor C1 raise the output voltage V 0 significantly from the source voltage, as shown in the equation below. When compared to a traditional inverter, the super-lift multilevel inverter (SLMLI) has benefits such as modularity, fewer components, the absence of additional clamping diodes, a lower number of switches, and the ability to quickly alter the number of output voltage levels.

Figure 16.3 depicts a 15-level super-lift inverter [16–20]. The period of switches turning ON and OFF in SLMLI can only be done once per

10.1002/9781119873266.ch16, Downloaded from https://onlinelibrary.wiley.com/doi/10.1002/9781119873266.ch16 by Tsinghua University Library, Wiley Online Library on [05/11/2022]. See the Terms and Conditions (https://onlinelibrary.wiley.com/terms-and-conditions) on Wiley Online Library for rules of use; OA articles are governed by the applicable Creative Commons License

Table 16.1 Design of PV array.

S. no.	Parameter	Range
1	Voltage at maximum power point	24 V
2	Total Power at MPP	0.5 kW
3	Current at MPP, $I_{mp} = P_{mp}/V_{mp}$ $I_{mp} = P_{mp}/V_{mp}$	0.08 A
4	No. of series connected module, $N_{Ser} = V_{mp}/V_{mpp}$ $N_{Ser} = V_{mp}/V_{mpp}$	cells

cycle. As a result, it simply addresses the switching loss problem. Each SLMLI produces seven different voltage outputs: (+E, 0, and–E), (+1E, 0, and –1E), (+2E, 0, and –2E) up to (+7E, 0, and –7E), etc. However, SLMLI produces stairway output voltage waveform that is measured. The output voltage waveform of a 15-level SLMLI value is seven times the input DC voltage [14]. There is a new way of achieving multilevel outputs using the SLMLI band inverter, which switches 10 capacitors in seven levels to achieve: E, 2E, 3E, 4E, 5E, 6E, and 7E. When duty cycle (k) = 6/7 (≈ 0.857) in 15-level SLMLI. Therefore, the operation of ON status is shown in Figure 16.3.

Each super-lift converter is nourished with the estimation of DC output voltage. The single-phase voltage of the inverter depends upon the band switching capacitor. The 15-level yield waveforms acquired by various switching combinations and switching pattern appeared in Table 16.2. Multistage centrifugal pumps that operate in a vertical position are known as electric submersible pumps. The load torque and motor speed of a water pump have a non-linear parabolic relationship. Liquids that are accelerated by the impeller lose their kinetic energy in the diffuser in which kinetic energy is converted to pressure. A mechanical coupling at the pump's base connects the pump shaft to the gas separator or protector.

An optional thrust bearing is used to support part of the axial forces in the pump but most of the thrust bearing is absorbed. The water pump has a parabolic nonlinear connection between load torque and speed, i.e., brake horsepower is the power to drive the pump [21–41].

$$\text{bhp} = \omega T \tag{16.1}$$

10.1002/9781119873266.ch16, Downloaded from https://onlinelibrary.wiley.com/doi/10.1002/9781119873266.ch16 by Tsinghua University Library, Wiley Online Library on [05/11/2022]. See the Terms and Conditions (https://onlinelibrary.wiley.com/terms-and-conditions) on Wiley Online Library for rules of use; OA articles are governed by the applicable Creative Commons License

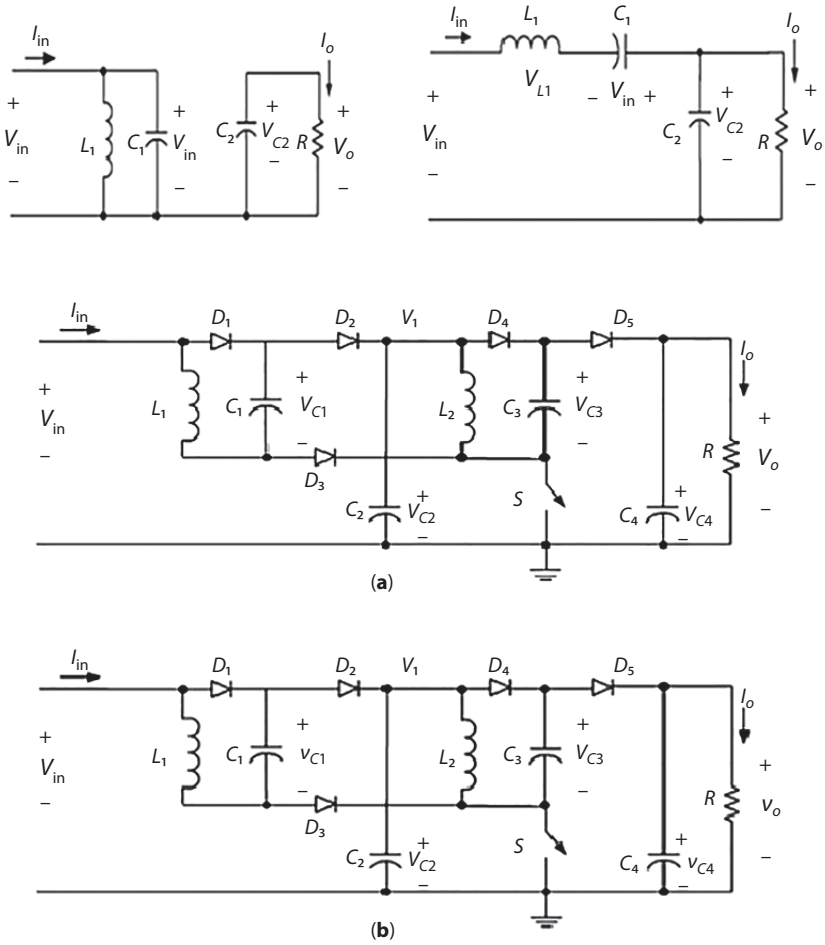


Figure 16.2 Double-lift circuit Luo converter. (a) Equivalent circuit for switch S is ON. (b) Switch S is OFF.

where is the shaft angular velocity and T is the shaft torque. If there were no losses, then P_w P_w and brake horse power would be equal, but, of course, P_w P_w is actually less and the efficiency of the power is defined as

$$\eta = \frac{P_w}{bhp} = \frac{\rho g Q H}{\omega T} \tag{16.2}$$

10.1002/9781119873266.ch16, Downloaded from https://onlinelibrary.wiley.com/doi/10.1002/9781119873266.ch16 by Tsinghua University Library, Wiley Online Library on [05/11/2022]. See the Terms and Conditions (https://onlinelibrary.wiley.com/terms-and-conditions) on Wiley Online Library for rules of use; OA articles are governed by the applicable Creative Commons License

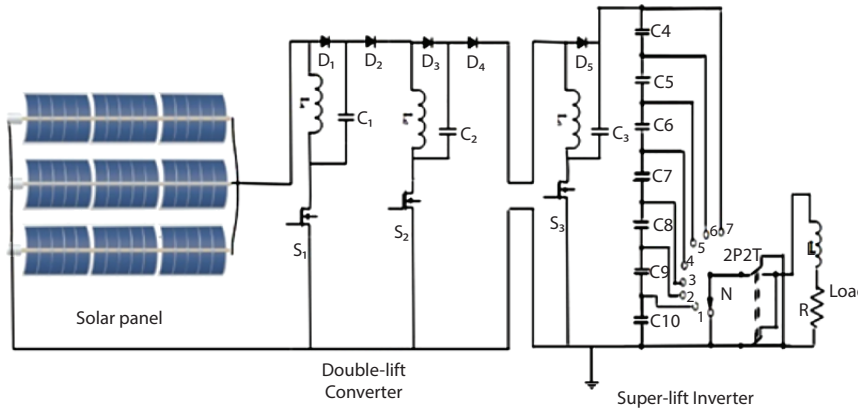


Figure 16.3 Circuit diagram for SLMLI (15 levels).

Table 16.2 Inverter switching method.

	Band switch position	Change over switch position	
		Switch ON state	Switch OFF state
1.	S_7	7E	−7E
2.	S_6	6E	−6E
3.	S_5	5E	−5E
4.	S_4	4E	−4E
5.	S_3	3E	−3E
6.	S_2	2E	−2E
7.	S_1	E	−E
8.	S_o	0	

16.4 Principle of Particle Swarm Optimization

PSO was learning from the problem-solving situation. In PSO, each solution is referred to as a "bird" in the search space. It is referred to as a "particle" by us. All particles have fitness values that are assessed by the fitness function in order to be optimized, as well as velocities that direct the particles' flight. The particles move through the problem space by following

10.1002/9781119873266.ch16, Downloaded from https://onlinelibrary.wiley.com/doi/10.1002/9781119873266.ch16 by Tsinghua University Library, Wiley Online Library on [05/11/2022]. See the Terms and Conditions (https://onlinelibrary.wiley.com/terms-and-conditions) on Wiley Online Library for rules of use; OA articles are governed by the applicable Creative Commons License

the optimal particles at the time. Novel PSO approaches were developed in 2008 to identify the optimal switching angles for the multilevel converter.

The approaches generate the necessary fundamental voltage while avoiding the generation of lesser and higher order harmonics [16–20]. In fundamental swarm optimization, matching velocity of the social iteration is identified by the vector representation.

$$X1(K) = [X2(K), X2(K).....Xn(K)] \tag{16.3}$$

where X_n (k) represents a parameter of the problem that has to be optimized. Particle positions and boundary conditions are randomly generated and use in (16.4) and (16.5). At the time step k+1, the velocity of i_th particle is given by

$$V_i\ (k+1) = wV_i\ (k)+C1rand(x)\ ((P_i\ (best)(k)-X_i\ (k))/\Delta t+C2rand(x)\ ((Gbest)(k)-X_i\ (k))/\Delta t \tag{16.4}$$

where w is the component of inertia; C1 is the social and C2 the cognitive; Pi (best) is the best location ever for a particle; G best is the best position ever obtained during movement of the whole social population of a particular particle; Rand (x) is a uniform positive random number from 0 to 1. The new location of each particle is determined by following one iteration:

$$X_i\ (k + 1) = X_i(k) + V_i\ (k)\ \Delta t \tag{16.5}$$

The present speed is set to zero, and the new speed is assessed according to Equation (16.4), but a new location is evaluated using equation with the difference of the term (16.5). The particle swarm algorithm starts from the creation and assignment of the first particles [21]. The goal function is evaluated at every particle location and the best (lowest) function value and the optimal position is determined. It selects new speeds, based on the present speed, the optimal locations for the particles, and best places in its neighborhood. It then updates the particle positions iteratively to identify the optimal angle of switch in SLMLI and minimize THD percent in sequence. PSO changes the particle location on an iterative basis and its iterations continue until optimum values of the method are achieved, and then, a stop condition may be used.

10.1002/9781119872061.ch16, Downloaded from https://onlinelibrary.wiley.com/doi/10.1002/9781119872061.ch16 by Tsinghua University Library, Wiley Online Library on [05/11/2022]. See the Terms and Conditions (https://onlinelibrary.wiley.com/terms-and-conditions) on Wiley Online Library for rules of use; OA articles are governed by the applicable Creative Commons License

16.5 Result and Discussion

The flowgraph of Genetic Algorithm for the proposed system is shown in Figure 16.4. The simulation results of Output voltage and current for the proposed 15-level super-lift Luo converter is appeared in Figure 16.5 and Figure 16.6. The THD results of Output voltage and current for the proposed 15-level super-lift Luo converter from simulation is shown in Figure 16.7 and Figure 16.8. The hardware model of concentrated SPV array with proposed converter is shown in Figure 16.9. The comparative analysis was carried out using simulation and hardware which is shown in Table 16.3.

The configuration of the proposed concentrated SPV module fed water pumping system is designed and simulated using MATLAB. The performance of the water pumping system using double-lift converter and SLMLI is evaluated using the simulation package, which gives the 15-level waveform for staircased Luo converter output voltage and current, as shown in Table 16.4. The output of SLMLIs includes harmonics, which may be

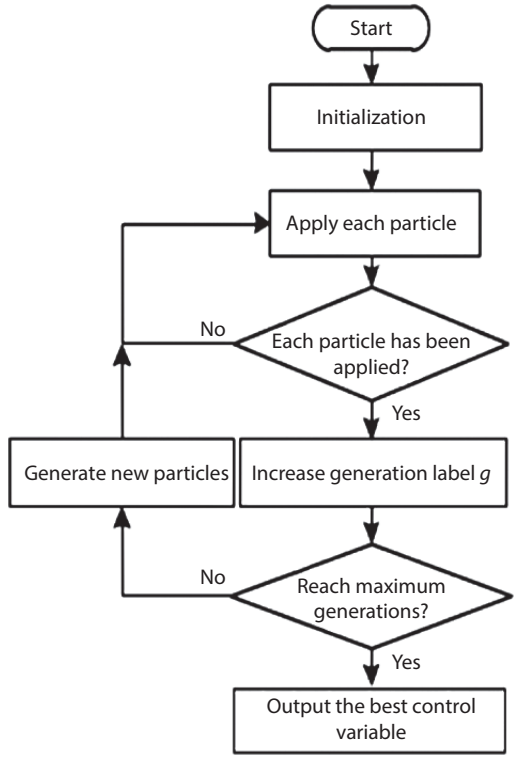


Figure 16.4 Flow chart for PSO algorithm.

10.1002/9781119873266.ch16, Downloaded from https://onlinelibrary.wiley.com/doi/10.1002/9781119873266.ch16 by Tsinghua University Library, Wiley Online Library on [05/11/2022]. See the Terms and Conditions (https://onlinelibrary.wiley.com/terms-and-conditions) on Wiley Online Library for rules of use; OA articles are governed by the applicable Creative Commons License

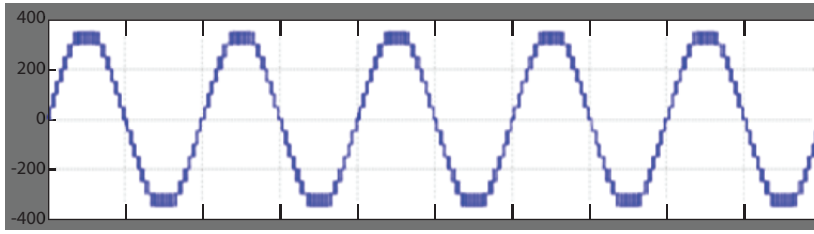


Figure 16.5 Simulation voltage waveform for 15-level super-lift Luo converter.

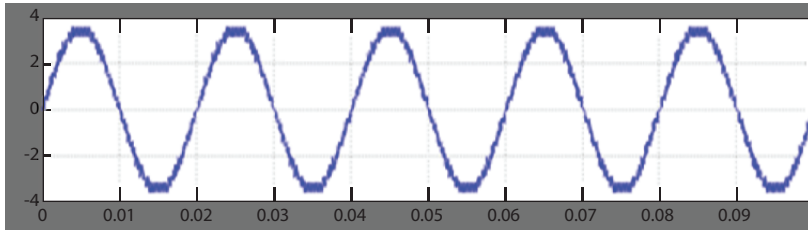


Figure 16.6 Simulation current waveform for 15-level super-lift Luo converter.

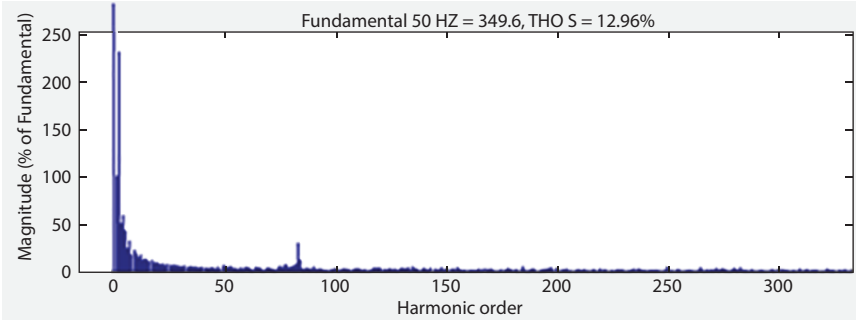


Figure 16.7 Harmonic order vs. magnetic phase output voltage.

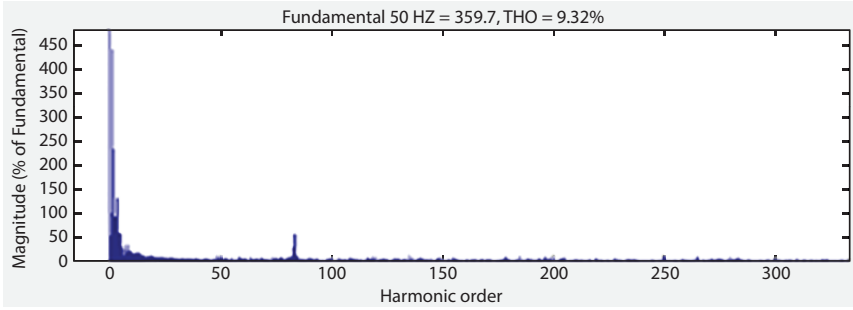


Figure 16.8 Harmonic order vs. magnetic phase output voltage.

10.1002/9781119872061.ch16, Downloaded from https://onlinelibrary.wiley.com/doi/10.1002/9781119872061.ch16 by Tsinghua University Library, Wiley Online Library on [05/11/2022]. See the Terms and Conditions (https://onlinelibrary.wiley.com/terms-and-conditions) on Wiley Online Library for rules of use; OA articles are governed by the applicable Creative Commons License

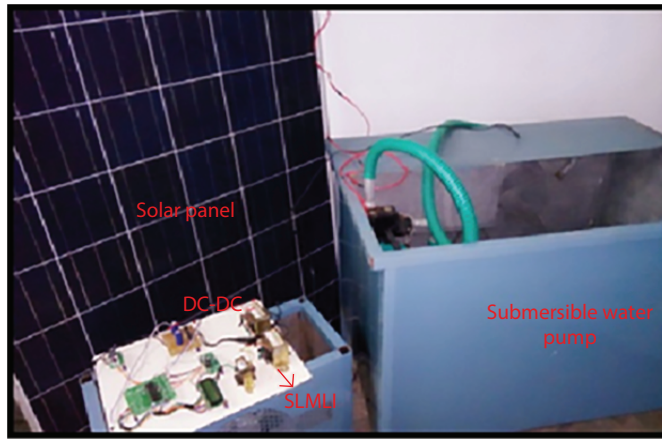


Figure 16.9 Hardware model of concentrated SPV array.

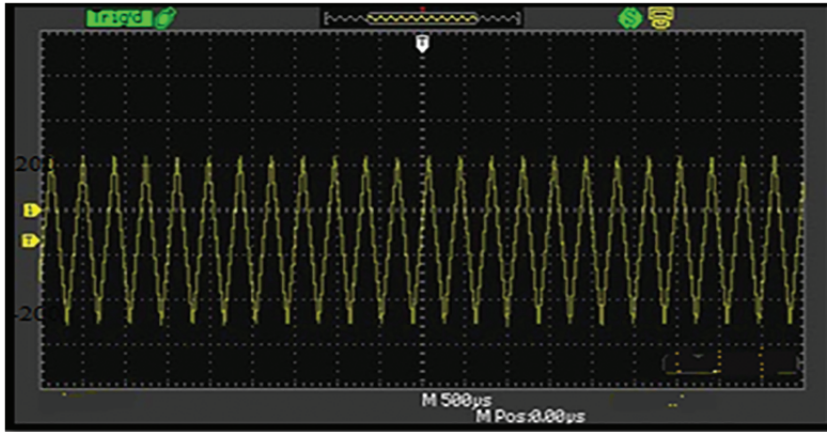


Figure 16.10 Hardware SLMLI voltage waveform.

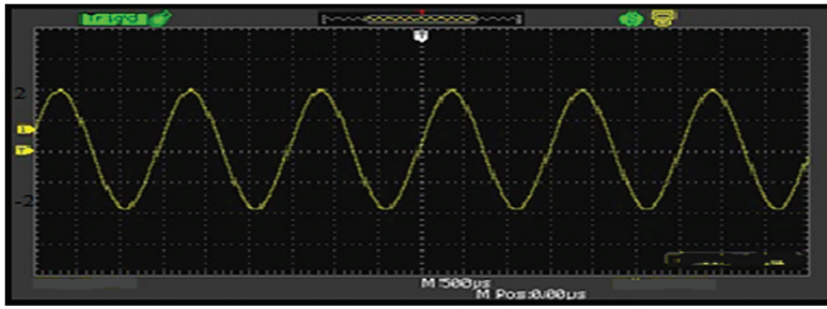


Figure 16.11 Hardware SLMLI current waveform.

10.1002/9781119873266.ch16, Downloaded from https://onlinelibrary.wiley.com/doi/10.1002/9781119873266.ch16 by Tsinghua University Library, Wiley Online Library on [05/11/2022]. See the Terms and Conditions (https://onlinelibrary.wiley.com/terms-and-conditions) on Wiley Online Library for rules of use; OA articles are governed by the applicable Creative Commons License

Table 16.3 Comparison of simulation and hardware result.

Simulation result			**Hardware result**		
THD%	V_{rms}	Amps	THD%	V_{rms}	Amps
9.32%	387 V	2.4 A	24.12%	240 V	1.8 A

Table 16.4 Specifications of proposed converter.

Circuit parameter (simulation)	
Output voltage, V_o	387 V
Output current, I_0	2.4 A
Voltage at maximum power point, V_{mpp} V_{mpp}	0.81*387 = 313.47 V
Current at maximum power point, I_{mpp} I_{mpp}	0.9*2.4 = 2.16 A
Capacitor (C_1 – C_{11}) C_1 – C_{11})	1,000e−6
Load resistance (RL)	100 Ω

measured using total harmonic distortion (THD). Using FFT analysis, it is a measure of the shape similarity between the waveform and the fundamental component.

Harmonic distortions are minimized in this case in relation to the magnetic phase output voltage. Except for the highest peak voltage, which is regulated by the PSO algorithm with a low THD percentage, other parameters of the solar module followed the atmospheric change. The output buffer is provided to an isolated circuit (optical isolator IC MCT2E) for each switch, and the hardware model is controlled and associated with the assistance of a PIC microcontroller child [22]. The output buffer is operated with an output frequency of 50 Hz and a carrier switching frequency of 10,000 Hz. Figures 16.10 and 16.11 demonstrate the submersible pump load output of 240 V and 1.8 A, respectively. The output line voltage waveform of the 15-level SLMLI is virtually sinusoidal, indicating that the submersible water pump method is effective. Concentrated PV (CPV) systems are specifically intended to provide water for irrigation in rural regions without access to power supply energy. Their main advantages of submersible water pumps are practically zero maintenance, in which they do not require fuel, contaminate, and finally are straight forward to install.

10.1002/9781119873266.ch16, Downloaded from https://onlinelibrary.wiley.com/doi/10.1002/9781119873266.ch16 by Tsinghua University Library, Wiley Online Library on [05/11/2022]. See the Terms and Conditions (https://onlinelibrary.wiley.com/terms-and-conditions) on Wiley Online Library for rules of use; OA articles are governed by the applicable Creative Commons License

16.6 Conclusion

Agriculture today suffers from multiple crises, and one of the worst crises is pertaining irrigation and water resources. The proposed system gives the basic principle of super-lift converters that is good for a small yard or for watering individual plants compare with diesel water pump. SPV panels are a low maintenance and environmentally friendly option for pumping irrigation water. The SLMLI has the simple structure and straight forward operation procedure, and easy control is used to construct higher level output voltage with reduced lower THD value. The proposed super-lift inverter with less number of semiconductor switches with minimum THD with the optimization control techniques such as PSO by using MATLAB/Simulink attains the value of THD 9.32% (simulation), and the appropriate prototype model THD is 24.12%. The drip irrigation must reduce water losses, without adding a substantial amount of head to the irrigated pumping system. It is also utilized to save installation space and costs.

References

1. Albert, J.R. and Stonier, A.A., Design and development of symmetrical super-lift DC–AC converter using firefly algorithm for solar-photovoltaic applications. *IET Circ. Device. Syst.*, 14, 3, 261–269, 2020. https://doi.org/10.1049/iet-cds.2018.5292.
2. Vanaja, D.S., Albert, J.R., Stonier, A.A., An experimental investigation on solar PV fed modular STATCOM in WECS using intelligent controller. *Int. Trans. Electr. Energy Syst.*, 13, e12845, 2021. https://doi.org/10.1002/2050-7038.12845.
3. Albert, J.R. and Vanaja, D.S., *Solar Energy Assessment in Various Regions of Indian Sub-continent, Solar Cells*, 1–14, 2021, DOI: 10.5772/intechopen.87735.
4. Kaliannan, T. *et al.*, Power quality improvement in modular multilevel inverter using for different multicarrier PWM. *EJECE*, 05, 02, 19–27, 2021, ISSN: 2736-5751. DOI: http://dx.doi.org/10.24018/ejece.2021.5.2.315.
5. Dhivya, M. and Renoald, A.J., Fuzzy grammar based hybrid split-capacitors and split inductors applied in positive output Luo-converters. *Int. J. Sci. Res. Sci. Eng. Technol.*, 3, 327–332, 2017. http://ijsrset.com/ IJSR SET173174.
6. Albert, J.R. *et al.*, Solar roadways-the future rebuilding infrastructure and economy. *Int. J. Electr. Electron. Res.*, 4, 2, 14–19, 2016. https://research publish.com/journal-details/IJEER.
7. Santhiya, K. *et al.*, Real time speed control of three phase induction motor by using lab view with fuzzy logic. *JSET*, 5, 2, 21–27, 2018. http://jset.sasapublications.com/wp-content/uploads/2018/04/1841019.pdf.

10.1002/9781119872061.ch16, Downloaded from https://onlinelibrary.wiley.com/doi/10.1002/9781119872061.ch16 by Tsinghua University Library, Wiley Online Library on [05/11/2021]. See the Terms and Conditions (https://onlinelibrary.wiley.com/terms-and-conditions) on Wiley Online Library for rules of use; OA articles are governed by the applicable Creative Commons License

8. Albert, J.R. *et al.*, Micro grid connected solar PV employment using for battery energy storage system. *J. Xidian Univ.*, 15, 3, 85–97, 2021. https://doi.org/10.37896/jxu15.3/010.
9. Kumarasamy, V., Ramasamy, V.K., Chinnaraj, G., Systematic design of multi-objective enhanced genetic algorithm optimized fractional order PID controller for sensorless brushless DC motor drive. *Circuit World*, 2021. https://doi.org/10.1108/CW-07-2020-0137
10. Vanchinathan, K. and Valluvan, K.R., A metaheuristic optimization approach for tuning of fractional-order PID controller for speed control of sensorless BLDC motor. *J. Circuit. Syst. Comp.*, 27, 08, 1850123, 2018. https://doi.org/10.1142/S0218126618501232.
11. Vanchinathan, K., Valluvan, K.R., Gnanavel, C., Gokul, C., Design methodology and experimental verification of intelligent speed controllers for sensorless permanent magnet Brushless DC motor. *Int. Trans. Electr. Energy Syst.*, 9, e12991, 2021. https://doi.org/10.1002/2050-7038.12991.
12. Vanchinathan, K. and Valluvan, K.R., Tuning of fractional order proportional integral derivative controller for speed control of sensorless BLDC motor using artificial Bee colony Optimization technique, in: *Intelligent and Efficient Electrical Systems*, pp. 117–127, Springer, Singapore, 2018, https://doi.org/10.1007/978-981-10-4852-4_11.
13. Rajasekaran, P. and Vanchinathan, K., Improved performance of four switch three phase brushless DC motor using speed-current control algorithm. *Int. J. Comput. Appl.*, 68, 11, 1–7, 2013. DOI: 10.5120/11620-5237.
14. Vanchinathan, K. and Valluvan, K.R., A study of sensorless BLDC motor drives and future trends. *Asian J. Res. Soc. Sci. Humanities*, 6, 9, 1863–1887, 2016. DOI: 10.5958/2249-7315.2016.00912.6.
15. Chandrasekaran, G., Kumarasamy, V., Chinraj, G., Test scheduling of core based system-on-chip using modified ant colony optimization. *J. Eur. Systèm. Autom.*, 52, 6, 599–605, 2019.
16. Chandrasekaran, G., Karthikeyan, P.R., Kumar, N.S., Kumarasamy, V., Test scheduling of system-on-chip using dragonfly and ant lion optimization algorithms. *J. Intell. Fuzzy Syst.*, (Preprint), 1–13, 2021.
17. Vanchinathan, K. and Valluvan, K.R., Improvement of time response for sensorless control of BLDC motor drive using ant colony optimization technique. *Int. J. Appl. Eng. Res.*, 10, 55, 6, 2015.
18. Gnanavel, C. and A. Alexander, S., Experimental validation of an eleven level symmetrical inverter using genetic algorithm and queen bee assisted genetic algorithm for solar photovoltaic applications. *J. Circuit. Syst. Comp.*, 23, 13, 1850212–23, 2008.
19. Vanchinathan, K., Sathiskumar, P., Selvaganesan, N., A Metaheuristic optimization algorithm-based speed controller for brushless DC motor: Industrial case study, in: *Metaheuristic Algorithms in Industry 4.0*, pp. 189–216, CRC Press, 2021.

10.1002/9781119873266.ch16, Downloaded from https://onlinelibrary.wiley.com/doi/10.1002/9781119873266.ch16 by Tsinghua University Library, Wiley Online Library on [05/11/2022]. See the Terms and Conditions (https://onlinelibrary.wiley.com/terms-and-conditions) on Wiley Online Library for rules of use; OA articles are governed by the applicable Creative Commons License

20. Gnanavel, C., Kamalamoorthy, N., Prabhu, V., Assessment among Single and three Phase 14–Echelon cascaded multilevel inverter. *Int. J. Sci. Res. Publ.*, 3, 5, 1–8, 2013.
21. Vanchinathan, K. and Selvaganesan, N., Adaptive fractional order PID controller tuning for brushless DC motor using artificial bee colony algorithm. *Results Control Optimization*, 4, 100032, 2021.
22. Gnanavel, C., Khanna, P.S., Rajavelan, M., Vanchinathan, K., Gokul, C., Real time monitoring and controlling of boiler drum parameters using Internet of Things (IoT). *Test Eng. Manage.*, 82, 3, 2195–2198, 2020.
23. Kalavalli, C., Sachinamreiss, G.N., Ali, A.N., Performance enhancement of boost converter fed permanent magnet synchronous machine. *IOP Conference Series: Materials Science and Engineering*, vol. 937, p. 012015, 2020.
24. Udayakumar, M.D., Gowthaman, K.S., Prabhu, A., Ali, A.N., HERIC Inverter-A SEPIC based transformer-less converter design and simulation for isolated standalone PV system. *IOP Conference Series: Materials Science and Engineering*, vol. 937, p. 012031, 2020.
25. Vijayalakshmi, S., Sivaraman, P.R., Karthick, R., Ali, A.N., Implementation of a new Bi-directional switch multilevel inverter for the reduction of harmonics. *IOP Conference Series: Materials Science and Engineering*, vol. 937, p. 012026, 2020.
26. Subramanian, A.T.S., Priyadharsini, S., Palaniyappan, S., Ali, A.N., A novel IOT based domestic automation system for load monitoring and efficient control. *IOP Conference Series: Materials Science and Engineering*, vol. 937, p. 012028, 2020.
27. Praveen, A.A.A., Kumaran, M.M., Ali, A.N., Minimization of power factor penalty charges for non-linear domestic loads with IOT technology. *IOP Conference Series: Materials Science and Engineering*, vol. 937, p. 012011, 2020.
28. Sivamani, D., Ramkumar, R., Nazarali, A., Shyam, D., Design and implementation of highly efficient UPS charging system with single stage converter. *Mater. Today: Proc.*, 45, 2, 1809–1819, 2021, 10 October 2020.
29. Paveethra, S.R., Kalavalli, C., Vijayalakshmi, S., Ali, Dr. A. N., Shyam, D., Evaluation of voltage stability of transmission line with contingency analysis. *Int. J. Sci. Technol. Res.*, 9, 02, 4018–22, 2020.
30. Ali, A.N., Sivamani, D., Jaiganesh, R., Pradeep, M., Solar powered air conditioner using BLDC motor. *IOP Conference Series: Material and Science Engineering*, vol. 623, Oct 2019.
31. Venkatesh, V., Ali, A.N., Jaiganesh, R., Indragandhi, V., Extraction and conversion of exhaust heat from automobile engine in to electrical energy. *IOP Conference Series: Material and Science Engineering*, vol. 623, Oct 2019.
32. Shyam, D., Premkumar, K., Thamizhselvan, T., Ali, A.N., Priya, M.V., Symmetrically modified laddered H-bridge multilevel inverter with reduced configurational parameters. *Int. J. Eng. Adv. Technol.*, 9, 1, 5525–5532, Oct 2019.

10.1002/9781119873761.ch16, Downloaded from https://onlinelibrary.wiley.com/doi/10.1002/9781119873761.ch16 by Tsinghua University Library, Wiley Online Library on [05/11/2022]. See the Terms and Conditions (https://onlinelibrary.wiley.com/terms-and-conditions) on Wiley Online Library for rules of use; OA articles are governed by the applicable Creative Commons License

33. Ali, A.N., Jayabharath, R., Udayakumar, M.D., An ANFIS based advanced MPPT control of a wind-solar hybrid power generation system. *Int. Rev. Model. Simul. (IREMOS)*, 7, 4, 638–643, 2014.
34. Ali, A.N., Jayabharath, Dr. R., Priyadharshini, R.S., A Single phase high efficient transformer less inverter for PV grid connected power system using ISPWM technique. *Int. J. Appl. Eng. Res. (IJAER)*, 10, 9, 7489–7496, 2015.
35. Ali, A.N. and Jeyabharath, R., Ride through strategy for a three-level dual Z-source inverter using TRIAC. *Circuits Syst.*, 7, 11, 3911, 2016.
36. Ali, A.N. and Jayabharath, R., Performance enhancement of hybrid wind/photovoltaic system using Z source inverter with Cuk-sepic fused converter. *Res. J. Appl. Sci. Eng. Technol.*, 7, 19, 3964–3970, 2014.
37. Ali, A.N., Gowri, N., Scholor, P.G., Power factor correction based bridgeless single switch SEPIC converter fed BLDC motor. *Adv. Nat. Appl. Sci.*, 10, 3, 190–198, 2016.
38. Ali, A.N., Jeyabharath, R., Udayakumar, M.D., Cascaded multilevel inverters for reduce harmonic distortions in solar PV applications. *Asian J. Res. Soc. Sci. Humanities*, 6, 11, 703–705, 2016.
39. Subramanian, A.T.S., Sabarish, P., Ali, A.N., *A Power factor correction based canonical switching cell converter for VSI fed BLDC motor by using voltage follower technique*, IEEE xplore Digital Library, pp. 1–8, 2017.
40. Ganesh, R.J., Ali, A.N., Kodeeswaran, S., Karthikeyan, B., Nagarajan, L., IoT based water management system for highly populated residential buildings. *Int. J. of Disaster Recovery And Business Continuity*, 11, 01, 4018–22, Apr 2020.
41. Ali, A.N., Ganesh, R.J., Sivamani, D., Shyam, D., Solar powered highly efficient seven-level inverter with switched capacitors. *IOP Conference Series: Material and Science Engineering*, vol. 906, p. 17578981, Aug. 2020, doi: 1757899X.

10.1002/9781119873266.ch16, Downloaded from https://onlinelibrary.wiley.com/doi/10.1002/9781119873266.ch16 by Tsinghua University Library, Wiley Online Library on [05/11/2022]. See the Terms and Conditions (https://onlinelibrary.wiley.com/terms-and-conditions) on Wiley Online Library for rules of use; OA articles are governed by the applicable Creative Commons License